NASA TECHNICAL MEMORANDUM

NASA TM X-3175

NASA TM X-3175

EFFECT OF CASING TREATMENT ON PERFORMANCE OF A MULTISTAGE COMPRESSOR

Leon M. Wenzel, John E. Moss, Jr., and Charles M. Mehalic

Lewis Research Center
Cleveland, Ohio 44135

NATIONAL AERONAUTICS AND SPACE ADMINISTRATION • WASHINGTON, D. C. • JANUARY 1975

1. Report No.	2. Government Accession No.	3. Recipient's Catalog No.
NASA TM X-3175		

4. Title and Subtitle	5. Report Date
EFFECT OF CASING TREATMENT ON PERFORMANCE OF A MULTISTAGE COMPRESSOR	January 1975
	6. Performing Organization Code

7. Author(s)	8. Performing Organization Report No.
Leon M. Wenzel, John E. Moss, Jr., and Charles M. Mehalic	E-8085
	10. Work Unit No. 505-05

9. Performing Organization Name and Address	11. Contract or Grant No.
Lewis Research Center National Aeronautics and Space Administration Cleveland, Ohio 44135	
	13. Type of Report and Period Covered
12. Sponsoring Agency Name and Address National Aeronautics and Space Administration Washington, D. C. 20546	Technical Memorandum
	14. Sponsoring Agency Code

15. Supplementary Notes

16. Abstract

A J85-GE-13 engine was equipped with a compressor case which allowed changes to the case wall over the rotor tips of six of its stages. The engine was tested with four inlet configurations: undistorted and with 180° circumferential, hub radial, and tip radial distortions. Baseline data defining compressor performance and stall regions were taken for these inlet configurations with solid (untreated) compressor case inserts. Circumferentially grooved inserts were installed in the first three and last three stages, and the compressor was mapped under similar conditions. The compressor was mapped a third time with untreated inserts in the first three stages and inserts having slots conforming to blade angles in the last three stages. In most cases, the stall pressure ratio was the same as or lower than the baseline. Pumping capacity with the slotted inserts was reduced. Overall compressor efficiency with the grooved rings installed did not appreciably differ from the baseline, but it was 1 to 2 percentage points lower than the baseline with the slotted rings in place. Average stage characteristics for the undistorted inlet case showed little or no sensitivity to casing treatment.

17. Key Words (Suggested by Author(s))	18. Distribution Statement
Casing treatment Compressor stall Distortion	Unclassified - unlimited STAR Category 07 (rev.)

19. Security Classif. (of this report)	20. Security Classif. (of this page)	21. No. of Pages	22. Price*
Unclassified	Unclassified	29	$3.75

* For sale by the National Technical Information Service, Springfield, Virginia 22151

EFFECT OF CASING TREATMENT ON PERFORMANCE OF A MULTISTAGE COMPRESSOR

by Leon M. Wenzel, John E. Moss, Jr., and Charles M. Mehalic

Lewis Research Center

SUMMARY

A J85-GE-13 engine was equipped with a compressor case which allowed changes to the case wall over the rotor tips of six of its eight stages. The engine was run in an altitude facility with four inlet configurations: undistorted and with 180° circumferential, hub radial, and tip radial distortions. Compressor stalls were induced by closing the exhaust nozzle while holding corrected speed constant.

Baseline compressor maps were taken for the four inlet configurations with solid (untreated) compressor case inserts. Circumferentially grooved inserts were installed in the first three and last three stages, and the compressor was mapped under similar conditions. A third mapping was done with untreated inserts in the first three stages and inserts having slots conforming to blade angles in the last three stages.

In most cases, the stall pressure ratio was the same as or lower than the baseline. At 100 percent corrected rated speed with tip radial distortion, a small increase in stall pressure ratio was noted with both types of inserts. Pumping capacity with the slotted inserts and all inlet configurations was reduced. Overall compressor efficiency was not appreciably different with the grooved inserts installed, but was 1 to 2 percentage points lower with the slotted inserts in place. Most stalls occurred in the sixth or seventh stage for the baseline and the slotted inserts. The grooved inserts made the fifth stage a typical stall site. It was very difficult to locate the stall site precisely. Average stage characteristics for the undistorted inlet showed little or no sensitivity to casing treatment.

INTRODUCTION

Porous, slotted, and grooved casing treatments have been shown to have desirable effects on single-stage compressors (e.g., refs. 1 to 3). These casing treatments have

been effective in increasing the flow range, stall margin, and distortion tolerance of the compressor.

A program was started at the Lewis Research Center to extend these results to a multistage compressor. Because of the large amount of experience with the J85 at Lewis, this engine was chosen for the program.

An analytical study was made which showed that, if the casing treatment could modify the individual stage characteristics of the J-85 as it had in the single-stage compressor work, a gain in flow range would be realized (ref. 4).

This increase in flow range would serve to decrease the sensitivity of the compressor to inlet distortion. The study indicated that casing treatment applied to the front and rear stages would be beneficial.

To evaluate this prediction experimentally, Lewis contracted with the General Electric Company to design and fabricate a special compressor case for a J85-GE-13 engine. The case was equipped with removable inserts over the tips of the rotor blades of stages 1, 2, 3, 6, 7, and 8. Three sets of inserts were provided: one set was left untreated for baseline testing; one set was machined with circumferential grooves; and one set was machined with blade angle slots.

This report presents the results of an experimental program conducted with the engine installed in an altitude facility. The two types of casing treatment are compared with the baseline case at four corrected engine speeds (80, 87, 94, and 100 percent of rated) with the inlet undistorted and with 180° circumferential, hub radial, and tip radial distortions. Overall compressor maps are presented. Individual stage characteristics and overall compressor efficiency are compared for the various casing treatments with the undistorted inlet.

APPARATUS

Engine

The compressor case of a J85-GE-13 engine was redesigned to permit changes in the case wall over the rotor tips of the first three and last three of the eight stages. This was effected by providing segmented rings, T-shaped in cross section, which slipped into mating grooves in the compressor case. Figure 1(a) shows half of the compressor case with rings in place; figure 1(b) shows the case with the rings removed. The eighth-stage ring and groove are not apparent in these photographs; this ring is sandwiched between the compressor case and the main frame.

Three sets of rings were provided for testing. Two sets of rings were machined for different casing treatments; one set was left blank for baseline testing. A sketch of a typical grooved ring and dimensions for all the rings are presented in figure 2(a). The

grooves were circumferential and continued over the inner surfaces of the rings. Figure 2(b) shows a sketch and dimensions of the slotted ring. The angles of the slots were such that they were parallel to the chords of the rotor blades at their respective stages. Only the rear three stages were tested with slotted rings.

The design of the grooved and slotted casing treatments was based on the results of an experimental study in which casing treatment dimensions were systematically varied (ref. 5)

The variable inlet guide vanes of the engine were linked to compressor interstage bleed doors so that, when the guide vanes were fully closed, the bleed doors were fully open. These were operated according to the manufacturer's schedule; bleed doors varied linearly from fully open at a corrected engine speed of 80 percent to fully closed at 94 percent. The sensitivity of the bleed schedule to inlet temperature was removed. This allowed comparison of results without concern over inlet temperature.

Since this was a stall program, a first-stage turbine nozzle with approximately 74 percent nominal area was used. This nozzle allowed compressor stalls without excessive turbine temperatures.

The exhaust nozzle was manually controlled to effect compressor stall. Six blockage plates were added to the inner surface of the nozzle. With these in place, the range of nozzle area available was 400 to 1130 square centimeters.

The engine was tested without distortion and with three screen patterns at the inlet: 180° circumferential, tip radial, and hub radial. The screens were attached to a support structure located 44.1 centimeters upstream of the compressor face. Details of the support structure are given in reference 6.

The distortion screen used was a square grid made up of 0.081-centimeter wire spaced 0.282 centimeter apart, with approximately 50 percent blockage. The radial screen patterns covered 40 percent of the inlet area.

At a corrected engine speed of 100 percent typical distortions ((average high pressure - average low pressure)/average face pressure) of 12 to 13 percent were observed.

Instrumentation

The compressor face was instrumented with an array of 60 probes located 3.7 centimeters upstream of the compressor face. The array was made up of 12 rakes of five probes; the probes on each rake were area weighted radially. Inlet temperature was measured with 12 thermocouples located 7.9 centimeters upstream of the engine face.

Total-pressure and -temperature rakes were installed at the discharge of each compressor stage and were axially located at the leading edge of the stator blades and alined parallel to the blades. The rakes were made up of three probes, at 10, 50, and

90 percent of the immersion depth. Wall static-pressure taps were located at each stator row. Also, closely coupled, high-response pressure transducers at each stator row were provided to locate the sites of compressor stalls.

Compressor discharge instrumentation was installed through the four customer bleed ports at the rear of the compressor. At each port, three total-pressure, one static-pressure, and three total-temperature probes were used. A sketch of the pressure probes is shown in figure 3. The forward projection of the combustor prevented the building of the rake to span the entire flow stream. The arrangement of temperature probes was similar.

In the data reduction program, the interstage pressures and temperatures were averaged on an area-weighted basis to provide average stage discharge conditions. At the compressor discharge similar weightings were used: 20 percent for the inner probes, 60 percent for the middle probes, and 20 percent for the outer probes.

Engine airflow was calculated from pressures and temperatures measured in a plenum upstream of the inlet by using a previously determined inlet calibration.

PROCEDURE

Tests were conducted with ambient inlet temperature and a nominal inlet pressure of 6.6 newtons per square centimeter. These inlet conditions yielded a Reynolds number index of 0.65 to 0.70 at the compressor face. The altitude chamber was maintained at approximately 3.1 newtons per square centimeter to ensure a choked exhaust nozzle.

For each configuration of casing treatment, the compressor was mapped with an undistorted inlet and with screens designed to produce 180° circumferential, hub radial, and tip radial distortions. Each mapping consisted of four constant corrected speed lines (80, 87, 94, and 100 percent of rated). Several steady-state data points were taken along each speed line between those for wide-open exhaust nozzle area and stall.

As data were taken along the constant corrected speed lines, turbine discharge total temperature was observed on a control-room gage and recorded. This gage was watched carefully as the engine was stalled to obtain turbine discharge temperature at stall. Data obtained in this way were used to draw curves of compressor pressure ratio and corrected airflow as a function of turbine discharge temperature. These curves were extrapolated to the turbine discharge temperature at stall to determine compressor pressure ratio and corrected airflow at the stall point.

As stall was approached, an FM tape recorder was started to record data from the high-response interstage static-pressure transducers. These data were used to locate stall sites.

RESULTS AND DISCUSSION

Compressor Maps

Compressor maps for the untreated rings are presented in figure 4. In this figure, the open symbols represent data, the solid symbols are stall points extrapolated on the basis of turbine discharge temperature, and the lines are faired through the data. Data in this figure were corrected for errors in speed setting; for example, if a point was taken at 94.1 percent corrected speed instead of the desired 94.0 percent, pressure ratio and corrected airflow were adjusted by appropriate sensitivities.

The effect of inlet distortion is consistent with previous findings (ref. 5). The 180° circumferential distortion causes losses in stall pressure ratio at all speeds, particularly the higher two. Tip radial distortion also causes losses in stall pressure ratio. At the lower three speeds, an increase in pumping capacity is noted. Hub radial distortion has little effect on stall pressure ratio at the higher three speeds, and pumping capacity is reduced.

Figure 5 presents compressor maps taken with the circumferentially grooved rings installed in stages 1, 2, 3, 6, 7, and 8. The same procedures and distortion screens were used in obtaining these data as in obtaining those presented in figure 4. The lines in figure 5 represent untreated ring performance for the same conditions.

Except for a slightly higher stalling pressure ratio at 100 percent corrected speed with tip radial distortion and higher airflow at 94 percent corrected speed with the undistorted inlet, the performance with grooved rings is the same as or worse than the baseline performance.

Compressor maps taken with slotted rings in stages 6 to 8 are presented in figure 6. An improvement in stall pressure ratio at 100 percent corrected speed with tip radial distortion is noted. Pumping capacity is down for all distorted cases, although it is the same as that for the untreated rings with the undistorted inlet.

Figure 7 presents compressor efficiency as a function of corrected inlet airflow for the undistorted inlet with the three casing configurations. The efficiency is computed to account for bleed flow at the lower speeds. Only small differences in efficiency are noted between the untreated and grooved ring cases, but efficiency is 1 to 2 percentage points lower for the slotted ring case.

Stall Sites

A summary of stall sites is presented in table I. These stall sites were determined from recordings of the high-response interstage static-pressure transducers. The stage exhibiting the first drop in pressure is listed. The judgment of which pressure dropped

off first was often subjective; arguments could be made for two or more pressures. This ambiguity is indicated in the multiple entries appearing in the table. In three instances no determination of stall site could be made. Transient recordings were not available in two instances.

With untreated rings stalls occurred largely in stages 6 and 7, occasionally stage 5. However, with the grooved rings installed, most of the stalls occurred at stage 5. This fact suggests that an improvement in stall margin in the rear stages due to the treated rings had shifted in the stall site forward to the untreated stage 5. But this is not seen in the slotted ring data, which show stall occurring predominately in stages 6 and 7.

Stage Characteristics

Pressure and temperature characteristics for the individual stages are presented in figures 8 and 9, respectively. The flow coefficient is defined as

$$\varphi_i = \frac{V_{z,i}}{U_i}$$

The pressure coefficient is defined as

$$\psi_{P,i} = \frac{\gamma_{i-1}}{\gamma_{i-1} - 1} gRT_{i-1} \frac{\left(\frac{P_i}{P_{i-1}}\right)^{(\gamma_i - 1)/\gamma_i} - 1}{U_i^2}$$

The temperature coefficient is defined as

$$\psi_{T,i} = \frac{\gamma_{i-1}}{\gamma_{i-1} - 1} gRT_{i-1} \frac{\frac{T_i}{T_{i-1}} - 1}{U_i^2}$$

where

g gravitational constant, (kg)(cm)/(N)(sec^2)

i i^{th} stage conditions

P average total pressure, N/cm^2

R universal gas constant, (N)(cm)/(kg)(K)

T average total temperature, K

U rotor tip velocity, cm/sec

V_z axial flow velocity, cm/sec

γ ratio of specific heats

φ flow coefficient

ψ_P pressure coefficient

ψ_T temperature coefficient

The pressures and temperatures used to calculate these coefficients were averaged on an area-weighted basis. However, the calculation of average conditions at the compressor discharge with the 20-60-20 percent weighting described in the section Instrumentation is not really proper. In fact, any weighting assigned to these probes might be questioned.

As shown in figure 3, the innermost or "hub" probe lies near the center of the flow path. Readings from this probe could be more representative of average conditions than the weighted average. Accordingly, pressure and temperature characteristics for the eighth stage are presented for both weighted average and hub conditions. Although the differences are significant for the calculations across the eighth stage, the overall compressor parameters are only minutely affected.

In some instances, one or more pressure or temperature probes malfunctioned. The missing values were filled in by interpolation, by using a third-order polynomial least-squares fit.

The wide separations between the groups of data in the first-stage plots are caused by the variable inlet guide vanes: at 94 percent rated speed and above, the vanes were axial; at 87 percent rated speed, the vanes were nominally half closed; and at 80 percent rated speed, the vanes were fully closed.

A speed effect is evident for the other stages also. In the stages where different casing treatments were tested, the differences in the data due to speed are more profound than any difference due to casing treatment.

SUMMARY OF RESULTS

Compressor performance of a J85-GE-13 engine with two types of casing treatment was compared with that for the untreated case. Data were obtained for rotor speeds from 80 to 100 percent rated with no inlet distortion and with screen-induced 180° circumferential, hub radial, and tip radial distortions. The following results were ob-

tained:

1. Casing treatment was not effective in extending flow range or increasing stall margin.

2. Individual stage pressure and temperature coefficients were not appreciably affected by casing treatment.

Lewis Research Center,
National Aeronautics and Space Administration,
Cleveland, Ohio, October 8, 1974,
505-05.

REFERENCES

1. Osborn, Walter M.; Lewis, George W., Jr.; and Heidelberg, Laurence J.: Effect of Several Porous Casing Treatments on Stall Limit and on Overall Performance of an Axial-Flow Compressor Rotor. NASA TN D-6537, 1971.

2. Moore, Royce D.; Kovich, George; and Blade, Robert J.: Effects of Casing Treatment on Overall and Blade-Element Performance of a Compressor Rotor. NASA TN D-6538, 1971.

3. Bailey, Everett E.; and Voit, Charles H.: Some Observations of Effects of Porous Casings on Operating Range of a Single Axial-Flow Compressor Rotor. NASA TM X-2120, 1970.

4. Snyder, Roger W.; and Blade, Robert J.: Analytical Study of Effect of Casing Treatment on Performance of a Multistage Compressor. NASA TN D-6917, 1972.

5. Bailey, Everett E.: Effect of Grooved Casing Treatment on the Flow Range Capability of a Single-Stage Axial-Flow Compressor. NASA TM X-2459, 1972.

6. Calogeras, James E.; Mehalic, Charles M.; and Burstadt, Paul L.: Experimental Investigation of the Effect of Screen-Induced Total-Pressure Distortion on Turbojet Stall Margin. NASA TM X-2239, 1971.

TABLE I. - SUMMARY OF STALL SITES

Inlet distortion	Corrected engine speed, percent rated			
	80	87	94	100
	Stall site, stage			
Untreated rings				
None	5	(a)	6, 8	7
180° Circumferential	(b)	5, 6	6	6
Tip radial	6	7	6	(a)
Hub radial	(b)	5, 6	6	6, 7
Grooved rings in stages 1, 2, 3, 6, 7, and 8				
None	5	5	5	6
180° Circumferential	7	5	5	5
Tip radial	5	5	5	7
Hub radial	7	7	5	5
Slotted rings in stages 6, 7, and 8				
None	7	7	6, (b)	7
180° Circumferential	5, 6	5, 6, 7	6, 7	7, 8
Tip radial	(b)	7	7	6
Hub radial	(b)	5, 6	7	7

[a]Transient recordings were not available.

[b]Stall site could not be determined.

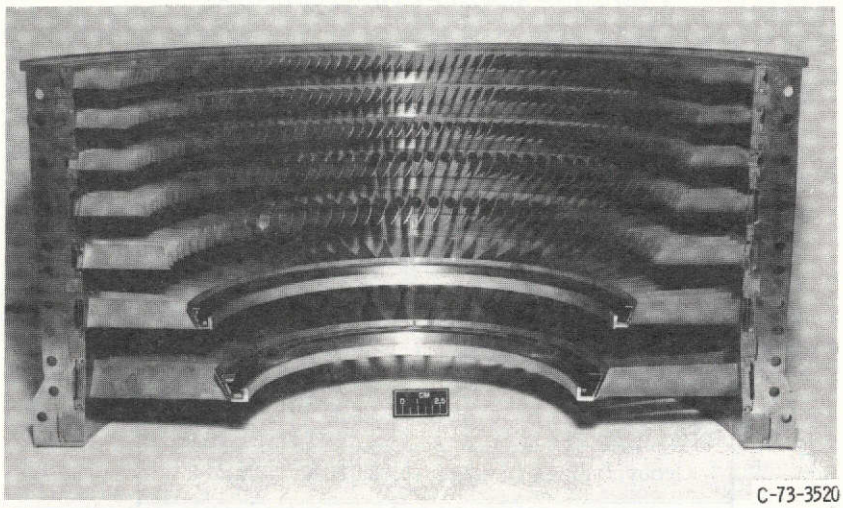

C-73-3520

(a) With inserts in place.

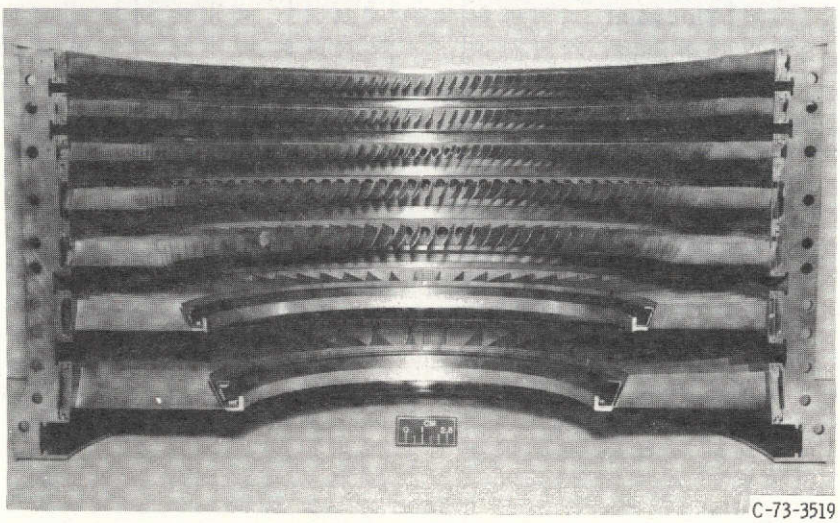

C-73-3519

(b) With inserts removed.

Figure 1. - Compressor case.

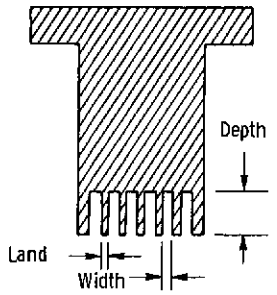

Stage	Number of grooves	Width, cm	Depth, cm	Land, cm
1	6	0.152	0.610	0.076
2	6	.102	.406	.051
3	6	.061	.229	.031
6	6	.051	.203	.025
7	5	.051	.203	.025
8	5	.051	.203	.025

(a) Grooved.

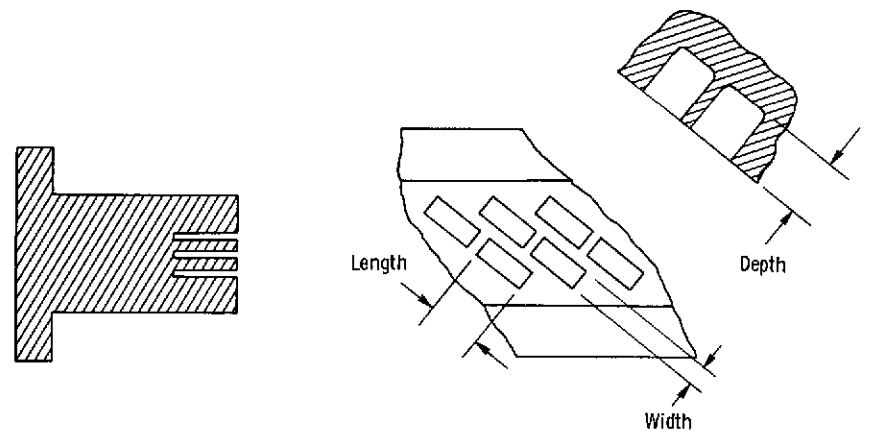

Stage	Number of pairs of slots	Width, cm	Length, cm	Depth, cm
6	512	0.102	0.267	0.305
7	522	.094	.226	.279
8	524	.089	.241	.254

(b) Slotted.

Figure 2. - Sketch and dimensions of rings.

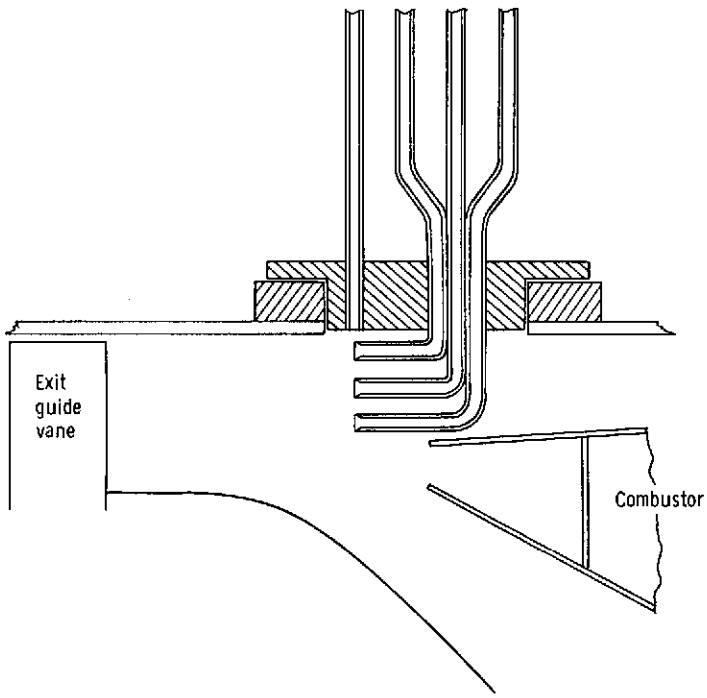

Figure 3. - Sketch of pressure probes at compressor discharge.

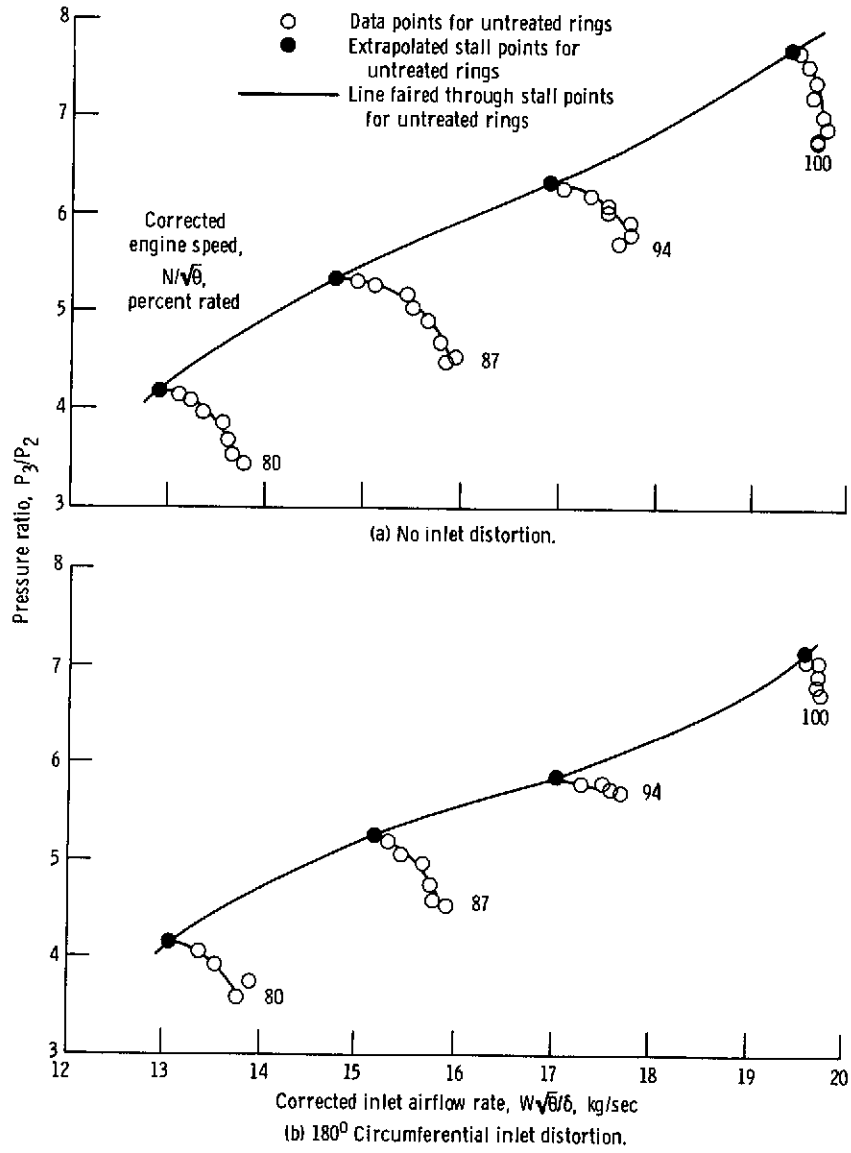

(a) No inlet distortion.

(b) 180° Circumferential inlet distortion.

Figure 4 - Baseline compressor performance.

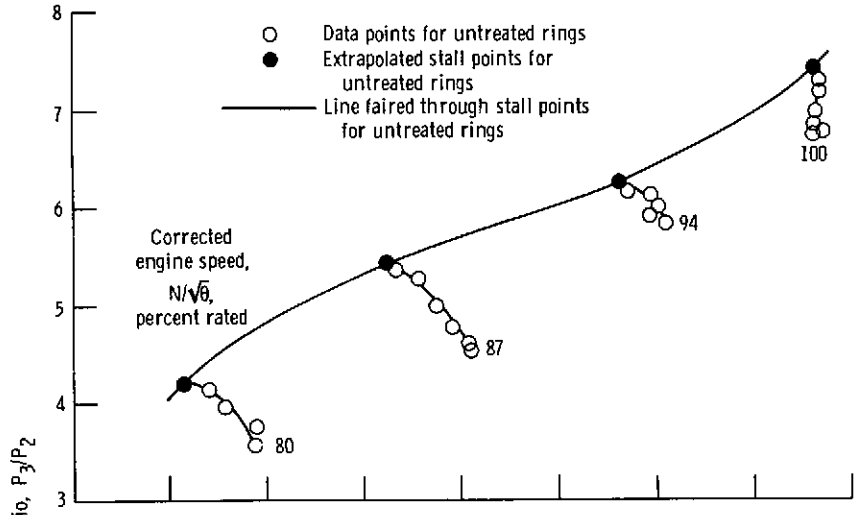

(c) Tip radial inlet distortion.

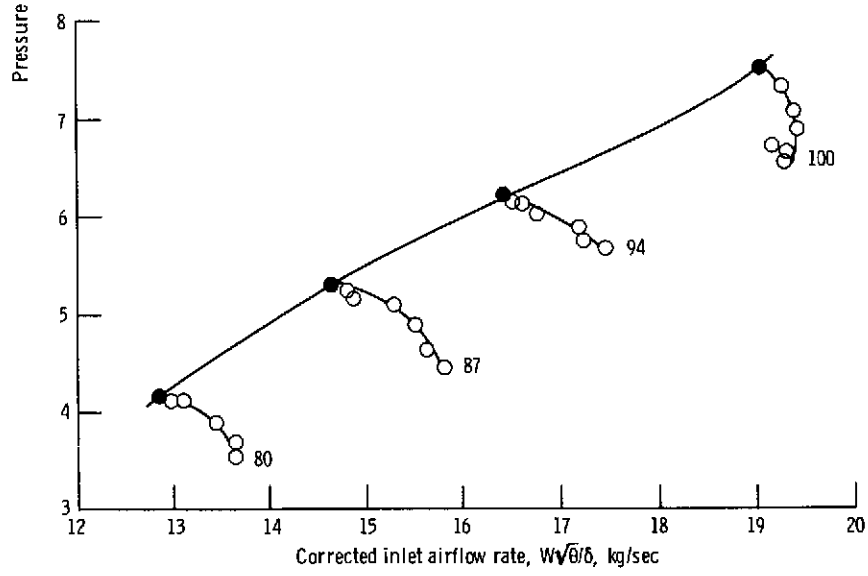

(d) Hub radial inlet distortion.

Figure 4. - Concluded.

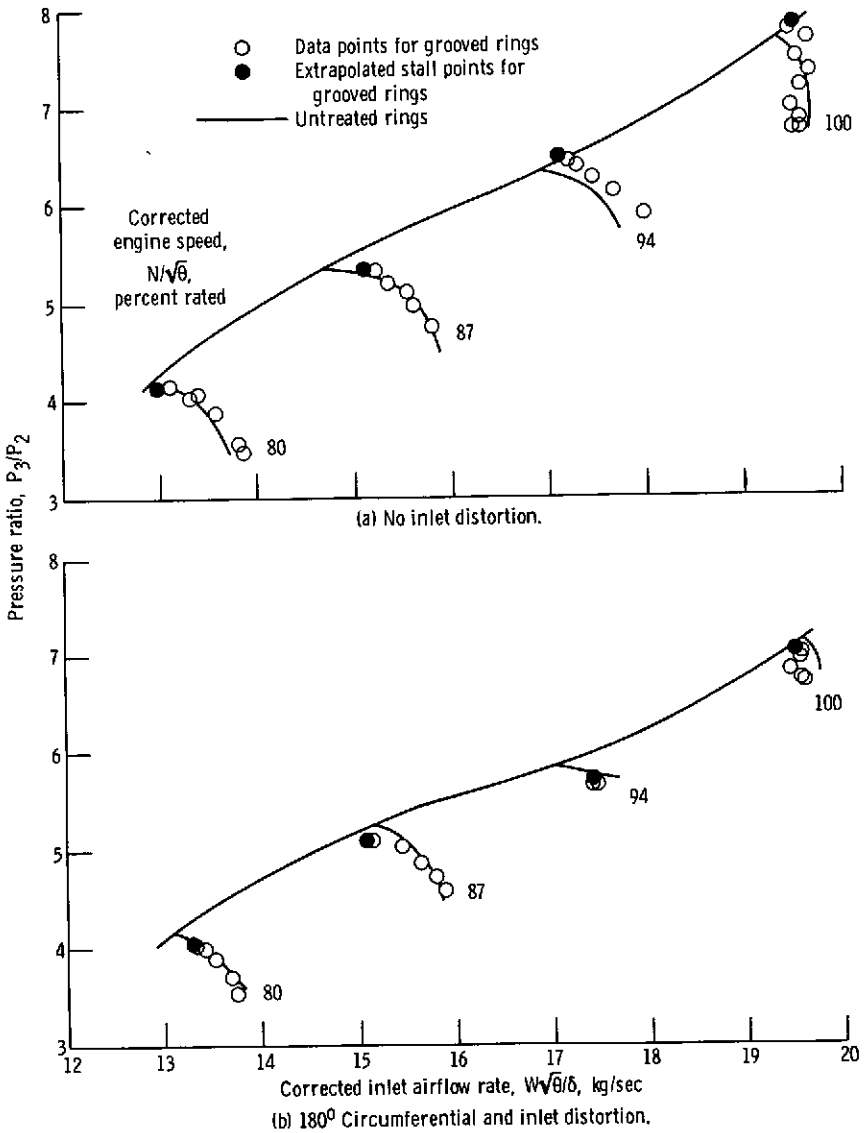

Figure 5. - Compressor performance with grooved rings in stages 1, 2, 3, 6, 7, and 8.

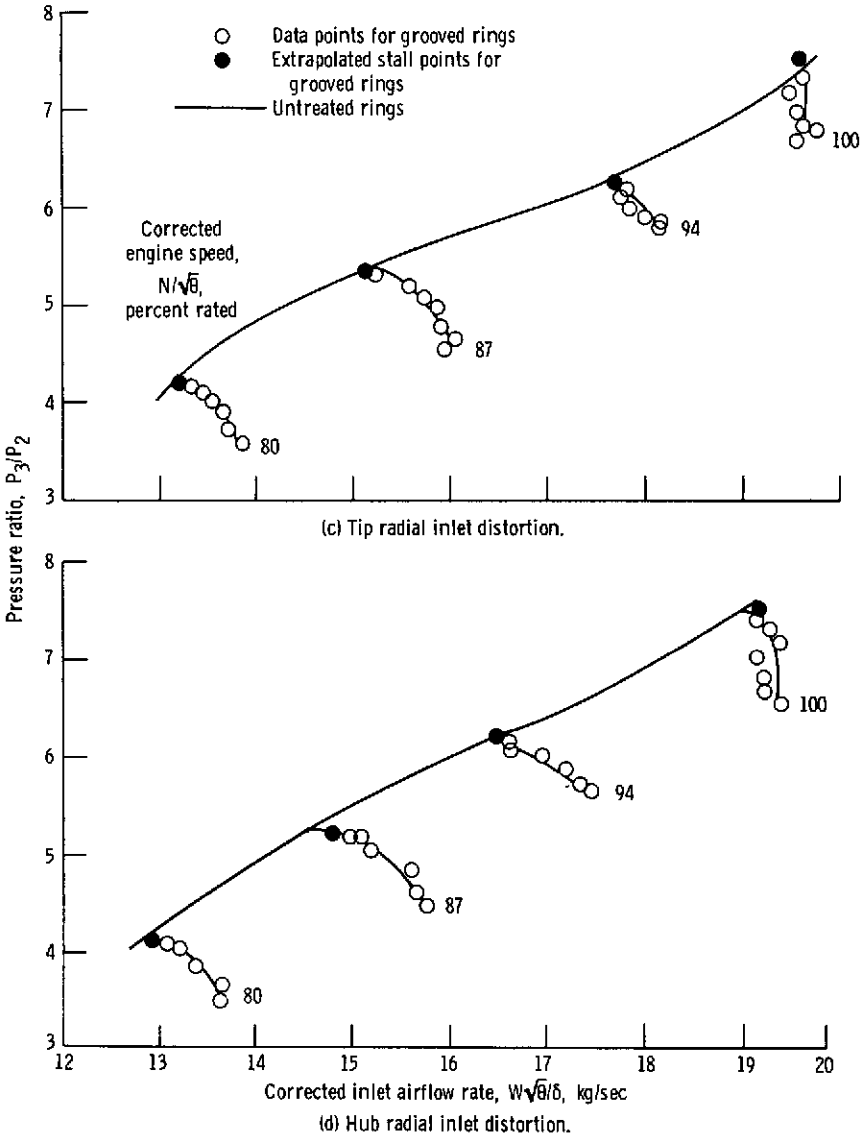

(c) Tip radial inlet distortion.

(d) Hub radial inlet distortion.

Figure 5. - Concluded.

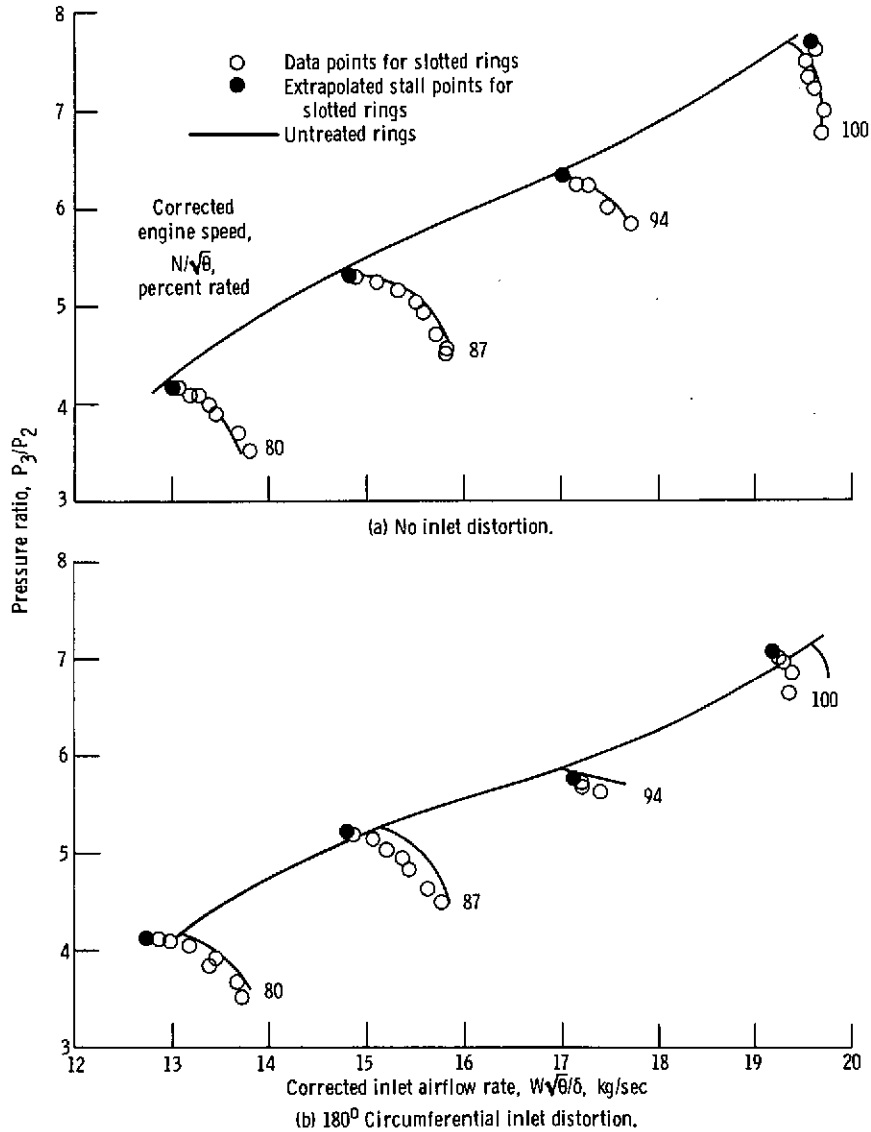

(a) No inlet distortion.

(b) 180° Circumferential inlet distortion.

Figure 6. - Compressor performance with slotted rings in stages 6, 7, and 8.

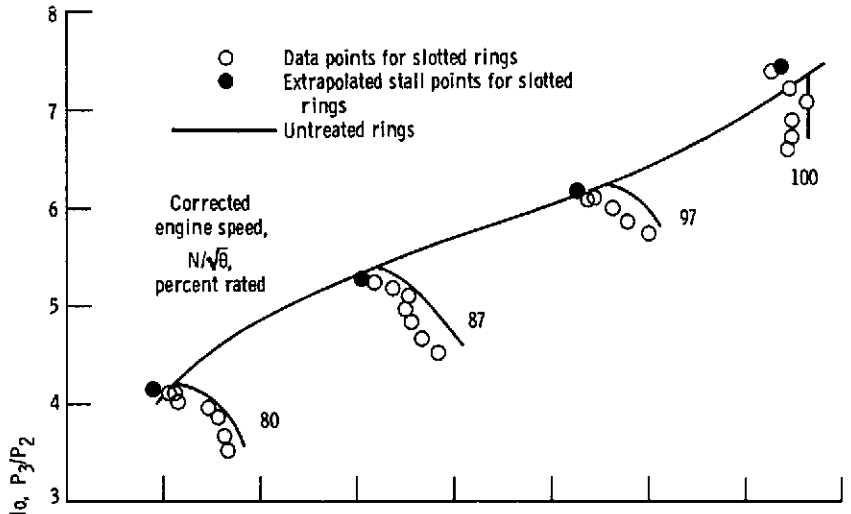

(c) Tip radial inlet distortion.

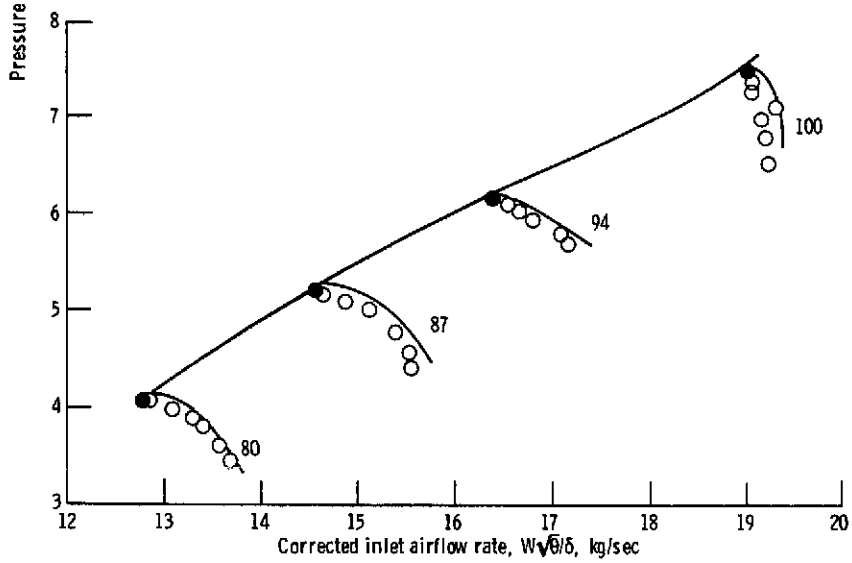

(d) Hub radial inlet distortion.

Figure 6. - Concluded.

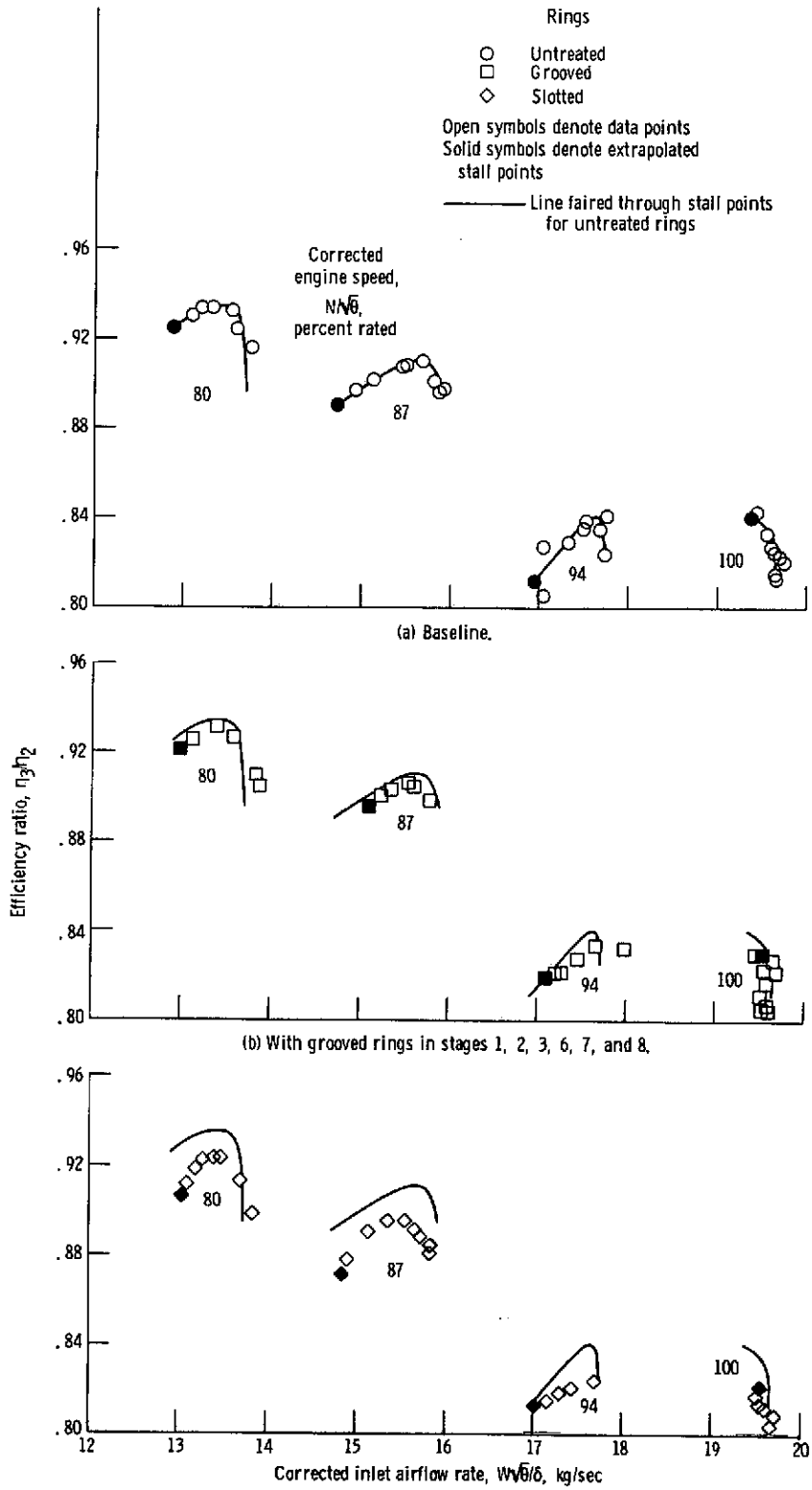

(a) Baseline.

(b) With grooved rings in stages 1, 2, 3, 6, 7, and 8.

(c) With slotted rings in stages 6, 7, and 8.

Figure 7. - Compressor efficiency.

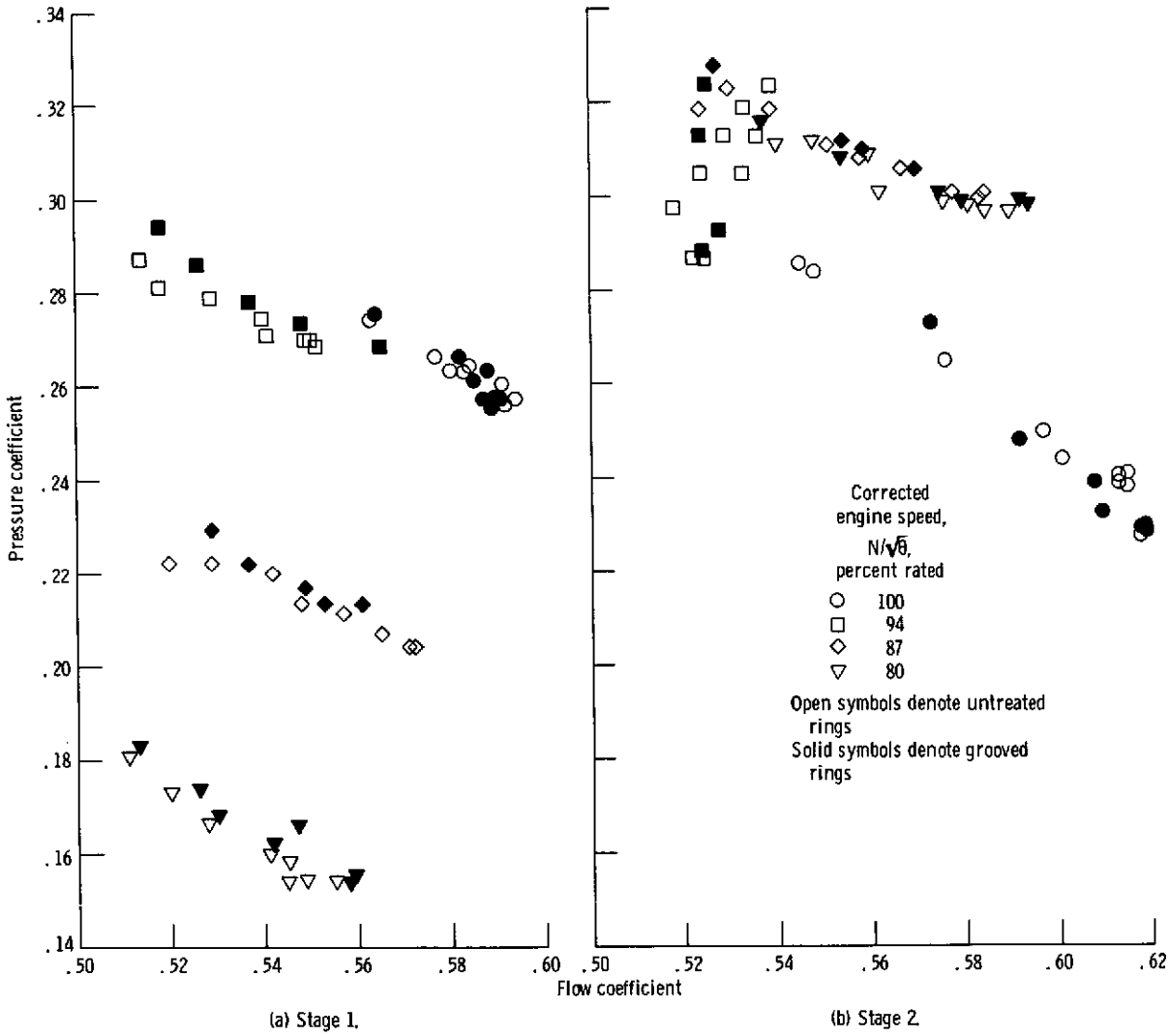

(a) Stage 1.

(b) Stage 2.

Figure 8. - Pressure characteristics for individual stages.

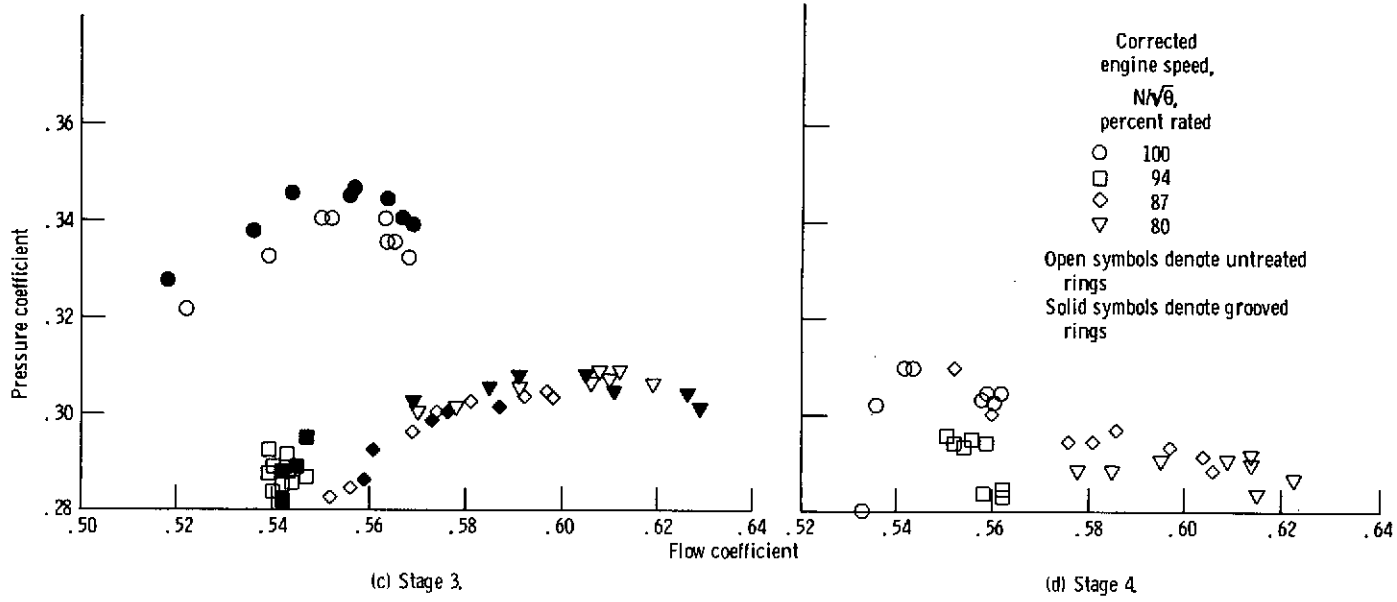

(c) Stage 3.

(d) Stage 4.

Figure 8. - Continued.

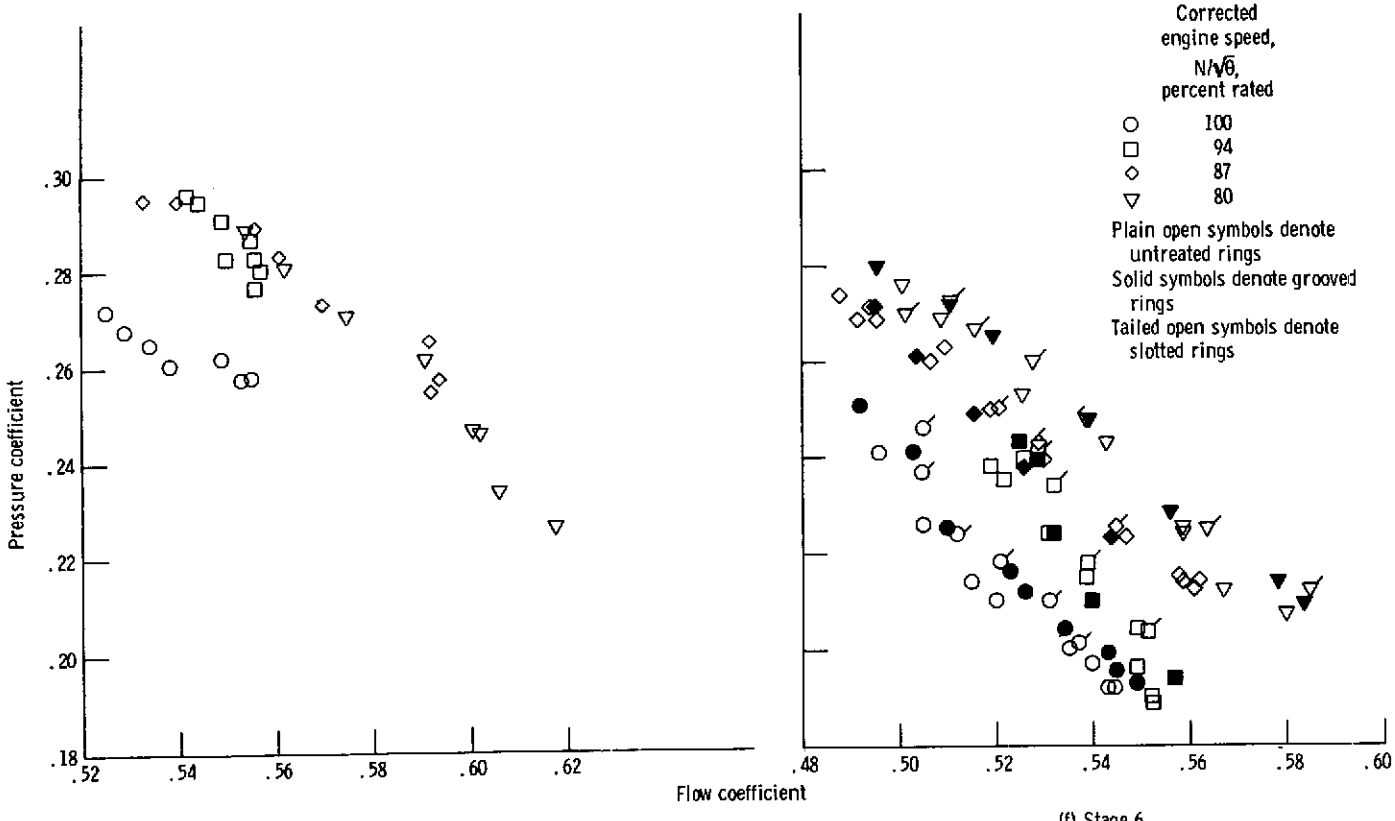

(e) Stage 5.

(f) Stage 6.

Figure 8. - Continued.

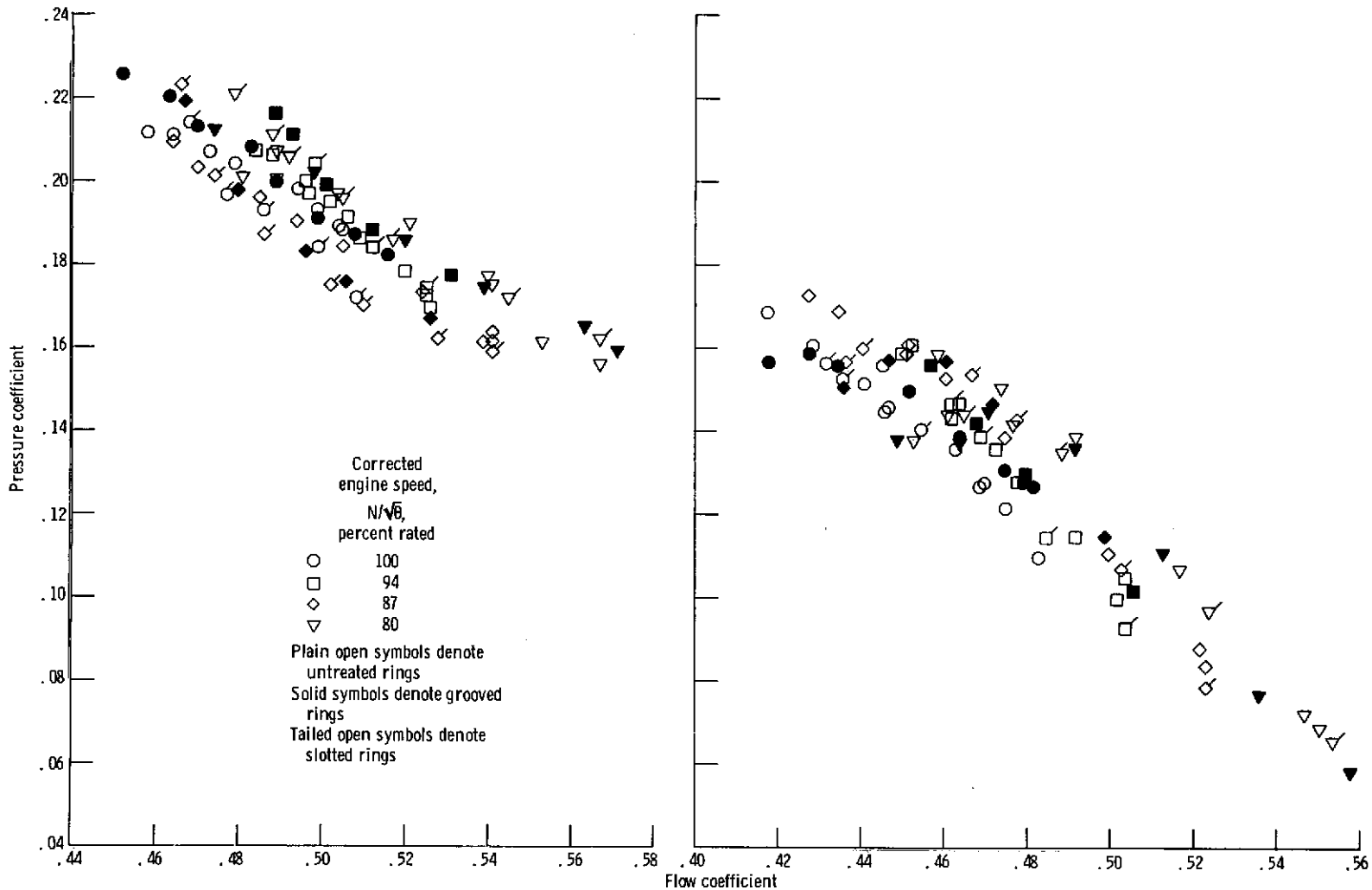

(g) Stage 7.

(h) Stage 8, average.

Figure 8. - Continued.

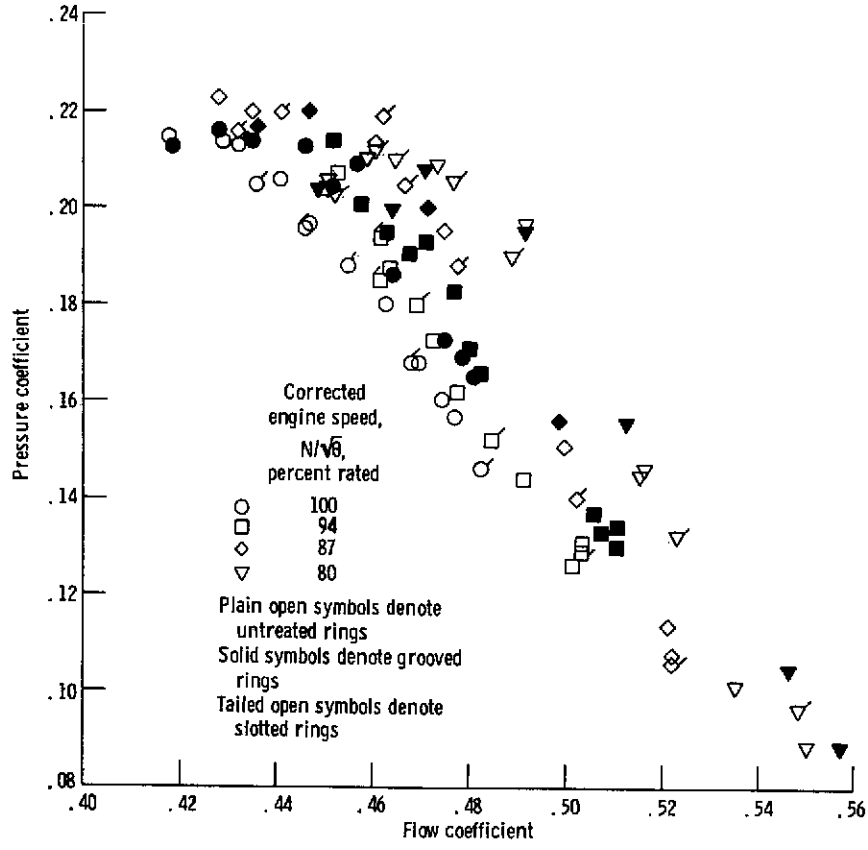

(i) Stage 8, hub.

Figure 8. - Concluded.

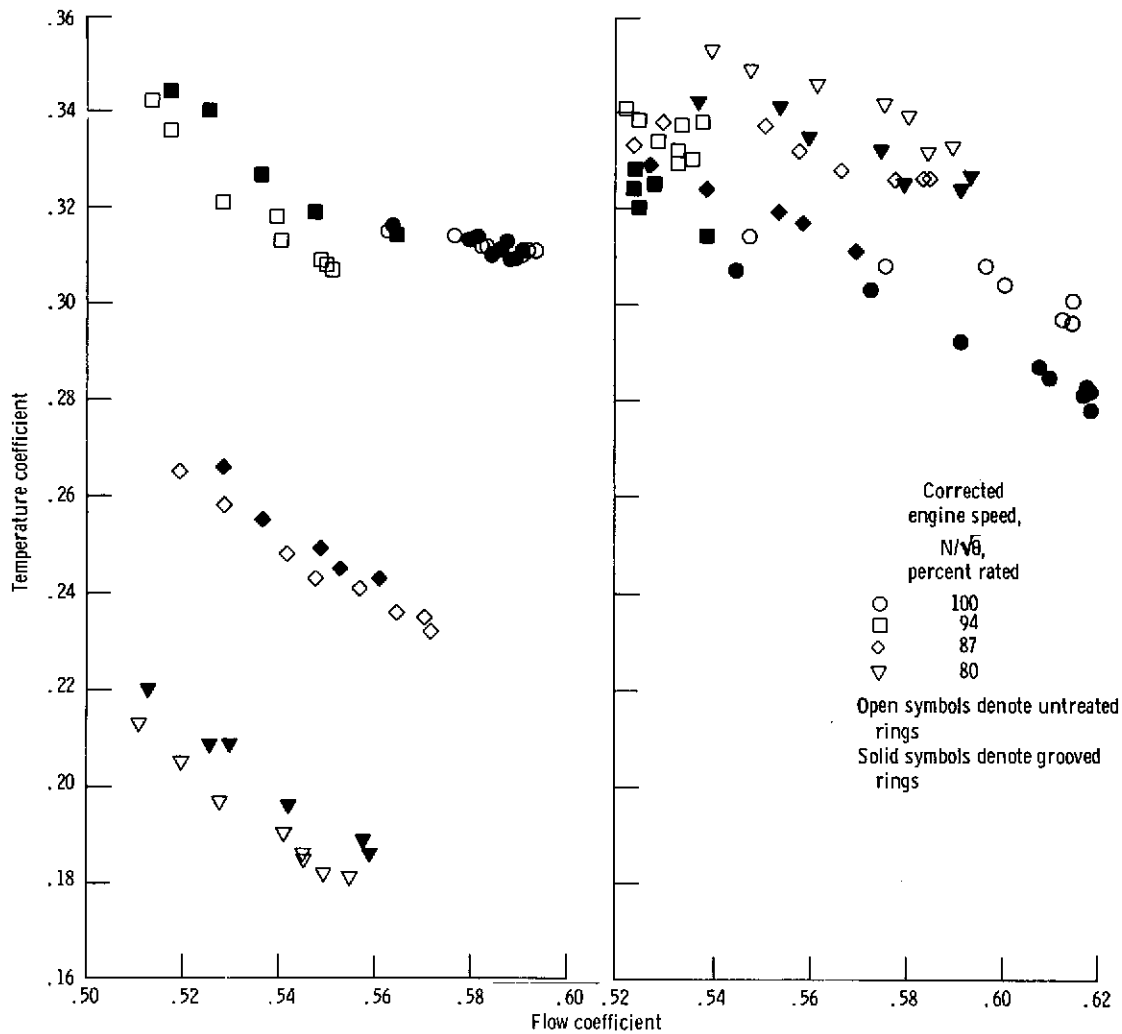

(a) Stage 1.

(b) Stage 2.

Figure 9. - Temperature characteristics for individual stages.

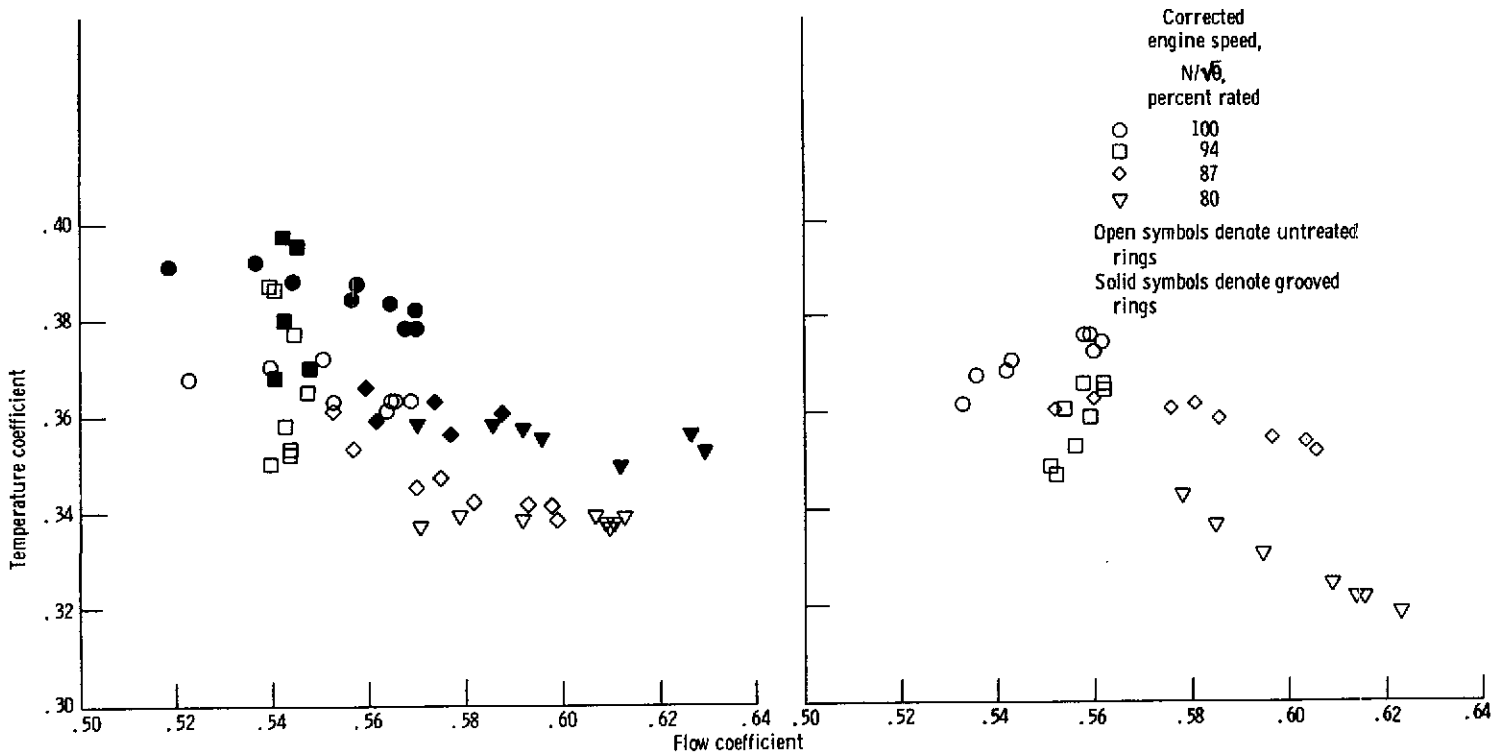

(c) Stage 3.

(d) Stage 4.

Figure 9. - Continued.

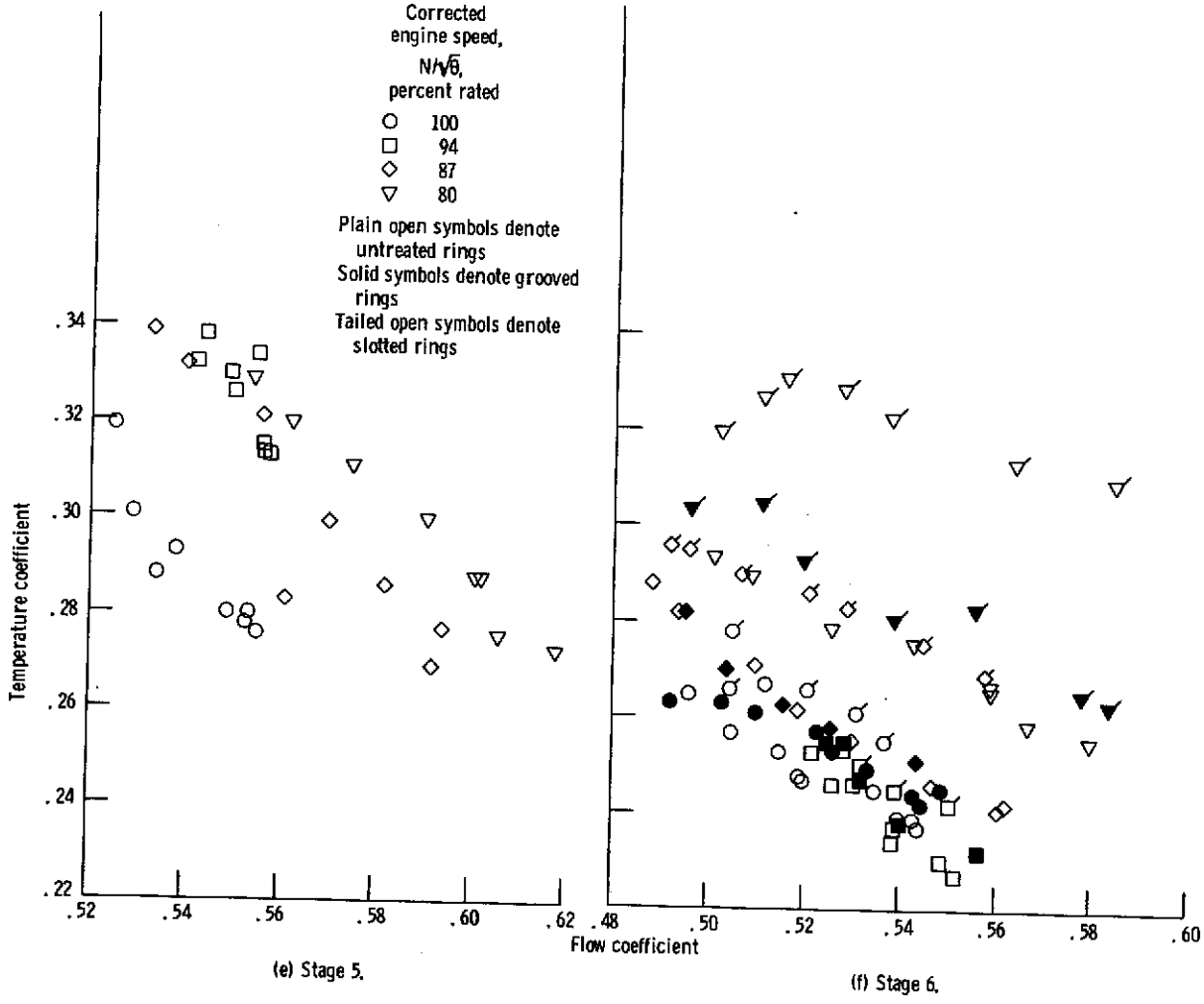

Figure 9. - Continued.

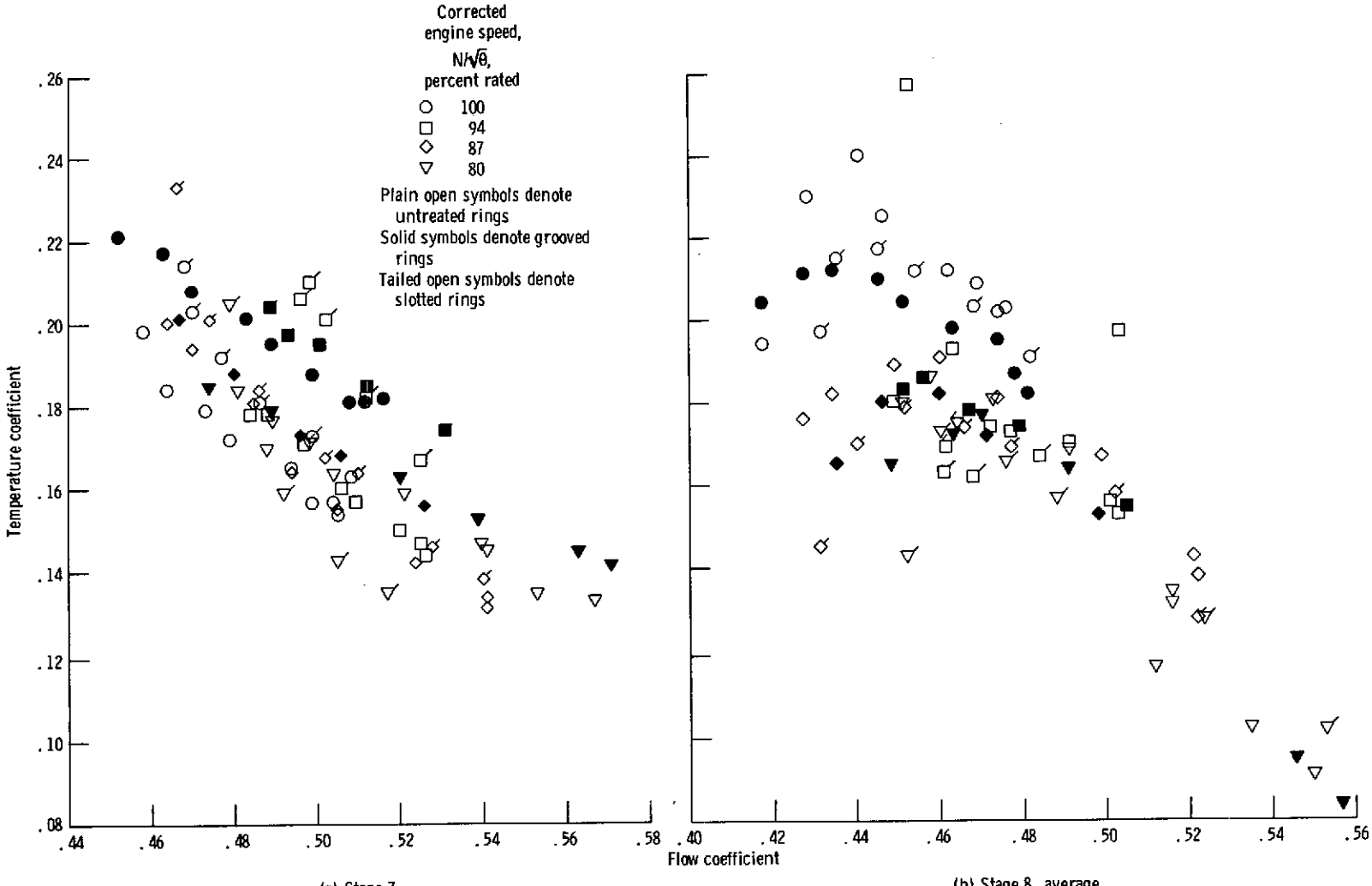

(g) Stage 7.

(h) Stage 8, average.

Figure 9. - Continued.

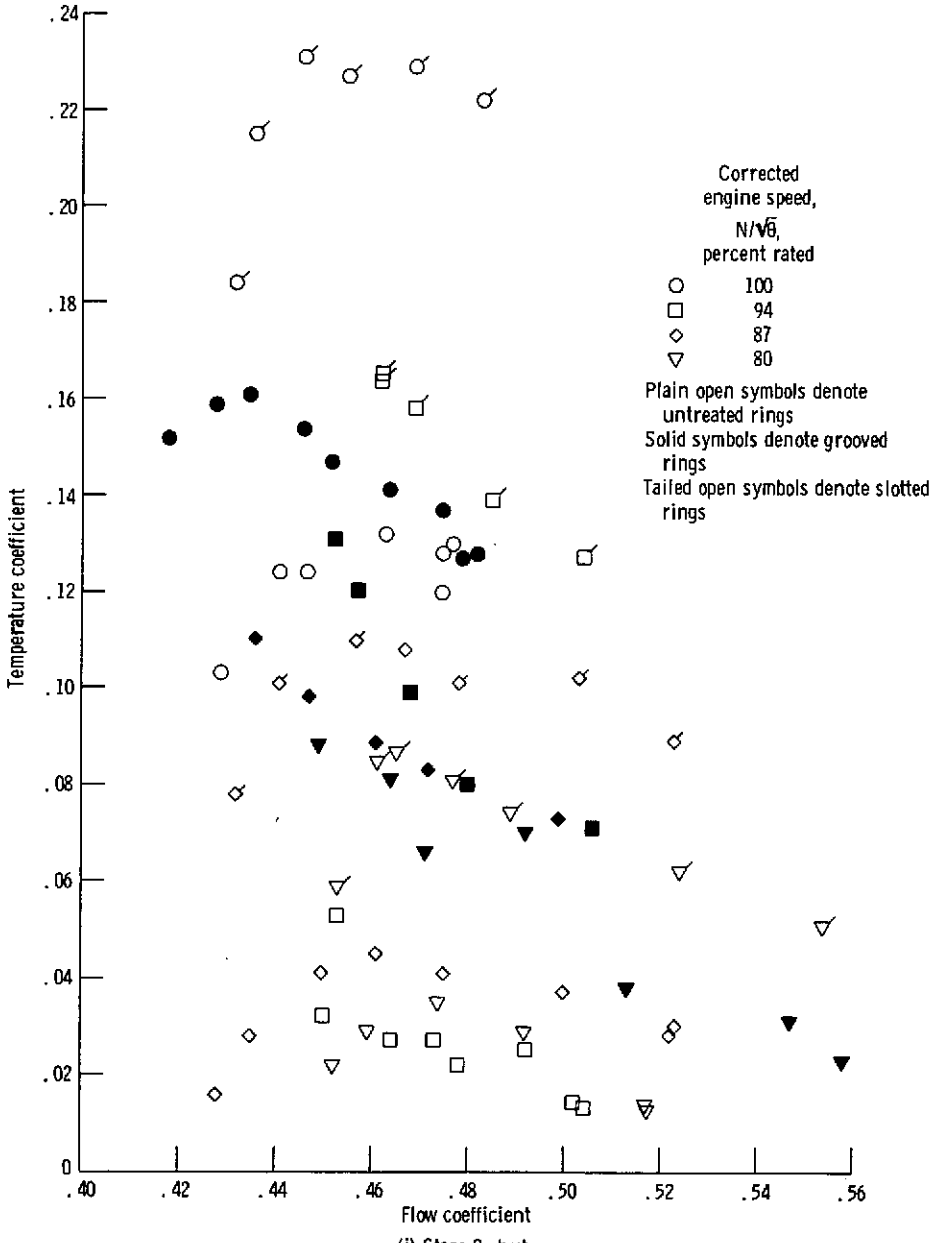

(i) Stage 8, hub.

Figure 9. - Concluded.